

3. E. H. Buhl, K. Halasy, P. Somogyi, *Nature* **368**, 823 (1994).
4. X.-G. Li, P. Somogyi, J. M. Tepper, G. Buzsáki, *Exp. Brain Res.* **90**, 519 (1992); X.-G. Li, P. Somogyi, A. Ylinen, G. Buzsáki, *J. Comp. Neurol.* **339**, 181 (1994).
5. D. D. Kunkel, J.-C. Lacaille, P. A. Schwartzkroin, *Synapse* **2**, 382 (1988); P. S. Buckmaster, B. W. Strowbridge, D. D. Kunkel, D. L. Schmiede, P. A. Schwartzkroin, *Hippocampus* **2**, 349 (1992); Z.-S. Han, E. H. Buhl, Z. Lorinczi, P. Somogyi, *Eur. J. Neurosci.* **5**, 395 (1993); K. Halasy and P. Somogyi, *ibid.*, p. 411; A. Gulyas *et al.*, *Nature* **366**, 683 (1993); A. Gulyas, R. Miles, N. Hajos, T. F. Freund, *Eur. J. Neurosci.* **5**, 1729 (1993); N. Tamamaki, K. Abe, Y. Nojyo, *Brain Res.* **452**, 255 (1988); N. Tamamaki and Y. Nojyo, *J. Comp. Neurol.* **291**, 509 (1990); *ibid.* **303**, 435 (1991).
6. A. Sik, M. Tamamaki, T. F. Freund, *Eur. J. Neurosci.* **5**, 1719 (1993).
7. D. G. Amaral and M. Witter, *Neuroscience* **31**, 571 (1989); F. H. Lopes da Silva, M. Witter, P. H. Boeijinga, A. Lohman, *Physiol. Rev.* **70**, 453 (1990).
8. S. R. Vincent and H. Kimura, *Neuroscience* **46**, 755 (1992).
9. The fimbria-fornix, the cingulate bundle, the supracallosal stria and part of the corpus callosum, and the cingulate cortex were removed by aspiration, leaving the dorsal hippocampus completely denervated from its subcortical inputs [G. Buzsáki, F. H. Gage, J. Czopf, A. Björklund, *Brain Res.* **400**, 334 (1987)].
10. H. H. Young, J. B. Furness, A. W. R. Shuttleworth, D. S. Bredt, S. H. Snyder, *Histochemistry* **97**, 375 (1992); J. G. Valtschanoff, R. J. Weinberg, V. N. Kharazia, M. Nakane, H. H. W. Schmidt, *J. Comp. Neurol.* **331**, 111 (1993).
11. Biocytin (3%) was injected extracellularly in the CA1 stratum oriens with micropipettes (resistance, 1 to 2 megohms) by 2.0- μ A depolarizing current pulses for 15 min in 20 urethane-anesthetized rats. Nine of the rats underwent fimbria-fornix lesion 7 to 20 days before the injection (9).
12. Rats were anesthetized with urethane. Stimulating electrodes were inserted into the ventral hippocampal commissure. Intracellular recording was carried out with glass micropipettes filled with biocytin solution (3% in 1 M potassium acetate; resistance, 60 to 95 megohms). After the physiological properties of the cell were determined, biocytin was injected with depolarizing current pulses (1 to 5 nA) for 5 to 60 min. After 2 to 16 hours, rats were perfused with a fixative (4). The avidin-biotinylated horseradish peroxidase complex reaction was used to visualize the biocytin-filled cells [K. Horikawa and W. Armstrong, *J. Neurosci. Methods* **25**, 1 (1988)]. Axon collaterals were drawn with the aid of a drawing tube (4, 6).
13. J. C. Lacaille, A. Mueller, D. D. Kunkel, P. A. Schwartzkroin, *J. Neurosci.* **7**, 1979 (1987); Y. Kawaguchi, H. Katsumaru, T. Kosaka, C. W. Heizmann, K. Hama, *Brain Res.* **416**, 369 (1987).
14. The sections were treated with 1% OsO₄ for 1 hour, dehydrated, counterstained with uranyl-acetate, and finally embedded in Durcupan (Fluka, Basel, Switzerland). Selected areas were re-embedded for ultrathin sectioning. Serial ultrathin sections were cut and mounted on single-slot Formvar-coated grids and counterstained with lead acetate (6).
15. G. Buzsáki, *Neuroscience* **31**, 551 (1989); T. H. Bullock, G. Buzsáki, M. C. McClune, *ibid.* **38**, 609 (1990); G. Buzsáki, Z. Horváth, R. Urioste, J. Hetke, K. Wise, *Science* **256**, 1025 (1992); A. Ylinen, A. Sik, A. Bragin, G. Jando, G. Buzsáki, *J. Neurosci.*, in press.
16. J. Holtsheimer and F. H. Lopes da Silva, *Exp. Brain Res.* **77**, 69 (1989); G. Buzsáki, M. Hsu, C. Slamka, F. H. Gage, Z. Horváth, *Hippocampus* **1**, 163 (1991).
17. R. J. Douglas and K. A. C. Martin, *Neural Comp.* **2**, 283 (1990); W. W. Lytton and T. J. Sejnowski, *J. Neurophysiol.* **66**, 1059 (1991).
18. T. J. O'Dell, R. S. Hawkins, E. R. Kandel, O. Arancio, *Proc. Natl. Acad. Sci. U.S.A.* **88**, 11285 (1991); E. M. Schuman and D. V. Madison, *Science* **254**, 1503 (1991); D. S. Bredt and S. H. Snyder, *Neuron* **8**, 3 (1992).
19. M. Zhuo, S. A. Small, E. R. Kandel, R. D. Hawkins,

- Science* **260**, 1946 (1993); E. M. Schuman and D. V. Madison, *ibid.* **263**, 532 (1994).
20. R. S. Sloviter and G. Nilaver, *J. Comp. Neurol.* **256**, 42 (1987).
21. R. A. Nicoll, R. C. Malenka, J. A. Kauer, *Physiol. Rev.* **79**, 513 (1990).
22. Supported by NIH, the Human Frontier Science Pro-

gram, the Whitehall Foundation, and the Finnish and the Hungarian academies of sciences (F5531). We thank D. G. Amaral, P. Andersen, T. V. P. Bliss, T. F. Freund, M. Hsu, E. R. Kandel, P. A. Schwartzkroin, J. M. Tepper, and R. Traub for helpful suggestions.

29 December 1993; accepted 10 August 1994

Molecular Determinants of State-Dependent Block of Na⁺ Channels by Local Anesthetics

David S. Ragsdale, Jancy C. McPhee, Todd Scheuer, William A. Catterall

Sodium ion (Na⁺) channels, which initiate the action potential in electrically excitable cells, are the molecular targets of local anesthetic drugs. Site-directed mutations in transmembrane segment S6 of domain IV of the Na⁺ channel α subunit from rat brain selectively modified drug binding to resting or to open and inactivated channels when expressed in *Xenopus* oocytes. Mutation F1764A, near the middle of this segment, decreased the affinity of open and inactivated channels to 1 percent of the wild-type value, resulting in almost complete abolition of both the use-dependence and voltage-dependence of drug block, whereas mutation N1769A increased the affinity of the resting channel 15-fold. Mutation I1760A created an access pathway for drug molecules to reach the receptor site from the extracellular side. The results define the location of the local anesthetic receptor site in the pore of the Na⁺ channel and identify molecular determinants of the state-dependent binding of local anesthetics.

Voltage-gated Na⁺ channels are integral membrane proteins that are responsible for the initial, rapid depolarization of the action potential in nerve and muscle cells. At negative membrane potentials, most Na⁺ channels are in closed, resting states. In response to membrane depolarization, the channels open in a few hundred microseconds, resulting in Na⁺ influx through a Na⁺-selective pore, and then convert to a nonconducting inactivated state. The rat brain Na⁺ channel consists of α (260 kD), β 1 (36 kD), and β 2 (33 kD) subunits (1). The α subunit is composed of four homologous domains (I through IV), each with six α -helical transmembrane segments (S1 through S6) (2, 3). The α subunit forms functional channels when expressed in mammalian cells (4, 5) or *Xenopus* oocytes (6), although coexpression of β 1 is required for normal kinetic properties in oocytes (7).

Local anesthetics block Na⁺ channels with complex voltage- and frequency-dependent properties that are important for the clinical efficacy of the drugs and that indicate that drug binding is modulated by channel state (8–11). The state-dependence of block can be explained by an allosteric model in which a modulated drug receptor has a higher affinity when channels are open or inactivated than when the channels are resting (8–10). Biophysical evidence is consistent with the hypothesis that this receptor site is on the α subunit in

the ion-conducting pore and accessible from the cytoplasmic side of the channel (9, 12–15). Determination of the amino acids that form the local anesthetic receptor site is important for understanding the complex action of these drugs. The S6 segment in domain IV (segment IVS6) of Ca²⁺ channels and the S6 segment of K⁺ channels have been implicated in the binding of pore blockers (16). We used site-directed mutagenesis to examine the function of segment IVS6 of the α subunit of the Na⁺ channel in local anesthetic action. Mutations in IVS6 altered the sensitivity of Na⁺ channels to local anesthetics, indicating that amino acids in this region are determinants of the action of these drugs.

Rat brain type IIA Na⁺ channels (3) expressed in *Xenopus* oocytes (wild type) (17, 18) were blocked ~40% by 200 μ M etidocaine, a tertiary amine local anesthetic, when the oocytes were stimulated infrequently (1 pulse per 20 s) (Fig. 1A). This tonic block mainly reflects drug binding to resting channels, the channel state that predominated at the holding potential of –90 mV (8–10). To determine whether amino acids in IVS6 are involved in local anesthetic action, we substituted alanine sequentially for the native amino acids at each position from F1756 to L1776 (Fig. 1A) (18). Alanine was chosen because it changes the size and chemical properties of the residues but has minimal effects on protein secondary structure (19).

Most IVS6 mutants exhibited a 40 to 50%

Department of Pharmacology, University of Washington, Seattle, WA 98195, USA.

tonic block by 200 μM etidocaine at a holding potential of -90 mV like wild type (Fig. 1A). However, mutants I1761A, F1764A, V1766A, V1767A, and N1769A displayed significantly altered sensitivity (Fig. 1A). N1769A was almost completely blocked by 200 μM etidocaine, whereas I1761A, V1766A, and V1767A were ~ 70 to 75% blocked. In contrast, F1764A was only inhibited 20%. The results suggest that the amino acids at these positions are determinants of local anesthetic binding to resting Na^+ channels. However, because of the state-dependent modulation of drug binding, it was also

possible that these effects were secondary to changes in the voltage dependence of inactivation rather than a reflection of actual changes in resting channel affinity. Therefore, to determine the mechanisms underlying the effects of these mutations, we examined the voltage dependence of tonic block over a broad range of holding potentials.

For the wild-type channel, in the absence of etidocaine, the relation between current amplitude and holding potential formed a characteristic inactivation curve with a midpoint ($V_{1/2}$) of about -54 mV (Fig. 1B). Etidocaine (200 μM) reduced

currents through wild-type channels at all voltages (Fig. 1B). Block was enhanced at depolarized holding potentials because of a greater availability of inactivated channels and was relieved at hyperpolarized holding potentials. At potentials more negative than -100 mV, the block approached a plateau of approximately 35% that was independent of holding potential. This indicates that inactivation was completely relieved at these potentials, so inhibition reflected only drug binding to resting Na^+ channels. The dependence of this resting block on etidocaine concentration was described by a 1:1 binding relation with a resting channel equilibrium dissociation constant (K_r) of 325 μM (Fig. 1D).

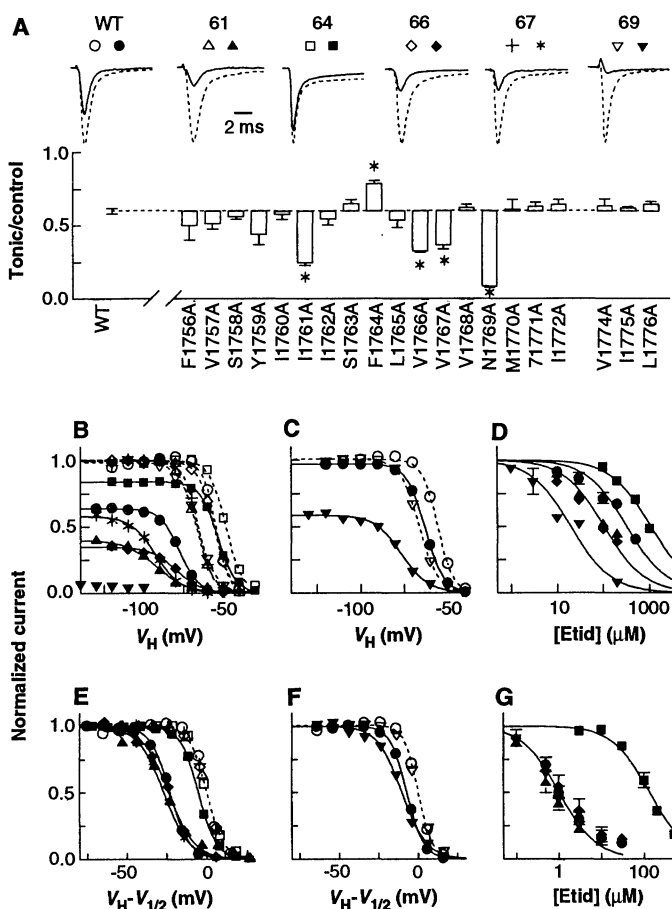
The control inactivation curve for V1766A was almost identical to that of wild-type channels (Fig. 1B). However, mutations I1761A, V1767A, and N1769A shifted $V_{1/2}$ negatively by 7 to 13 mV (Fig. 1B), whereas mutation F1764A shifted $V_{1/2}$ 8 mV positively (Fig. 1B). The negative shifts in $V_{1/2}$ for I1761A, V1767A, and N1769A increased the proportion of inactivated channels at moderate holding potentials, which could have caused part of the increased tonic block with these mutants. This was probably the main effect of V1767A because most of the increased block observed at -90 mV was relieved by strong hyperpolarization, and resting block was similar to wild type at -140 mV (Fig. 1B).

In contrast, resting block at the most negative membrane potentials for I1761A, V1766A, and N1769A was significantly greater than that of wild-type channels, indicating that these mutations altered the sensitivity of resting channels to etidocaine (Fig. 1, B through D). For I1761A and V1766A, resting block with 200 μM etidocaine was 55 to 60% (Fig. 1B), and K_r was ~ 100 μM (Fig. 1D). Mutant N1769A was almost completely blocked by 200 μM etidocaine at all potentials (Fig. 1B), and there was no detectable relief from block even when oocytes were held at -140 mV for up to 1 min. At a concentration of 10 μM etidocaine, block reached a plateau of about 40% at hyperpolarized potentials (Fig. 1C), indicating that the inhibition of Na^+ currents was due to an increased sensitivity of resting channels. K_r was 20 μM , a 15-fold increase in sensitivity as compared with wild-type channels (Fig. 1D).

In contrast to the mutations described above, F1764A caused a significant decrease in resting block. With 200 μM etidocaine, resting block was only 15% (Fig. 1B), and K_r was 1 mM, threefold greater than for wild-type channels (Fig. 1D).

The voltage dependence of tonic block resulted in a concentration-dependent negative shift ($\Delta V_{1/2}$) in the midpoint of inactivation

Fig. 1. Mutations in IVS6 alter tonic block by etidocaine. **(A)** Typical current records for wild-type (WT) and selected mutants in control (dashed lines) and 200 μM etidocaine (solid lines) experiments are shown above the histogram. Unless indicated, all currents were elicited by 15-ms pulses to 0 mV. The histogram shows mean amplitudes of currents \pm SEM ($n = 3$ to 28) for wild-type and mutant channels after block by 200 μM etidocaine. The data were normalized with respect to control currents elicited before drug application and plotted as deviations from the wild-type mean (dashed line). The asterisks show means that were significantly different from wild type [Student's t test; $P < 0.05$]. For N1769A, activation was shifted positively by 20 mV, so currents were evoked by pulses to $+20$ mV. **(B and C)** We assessed the voltage dependence of tonic block by test pulses applied after stepping to various holding potentials for 10 s. Peak currents were plotted as a function of holding potential (V_H). Each set of symbols represents data from a representative oocyte in control conditions and after application of 200 (B) or 10 (C) μM etidocaine for wild type (control, \circ ; with etidocaine, \bullet), I1761A (Δ , \blacktriangle), F1764A (\square , \blacksquare), V1766A (\diamond , \blacklozenge), V1767A ($+$, $*$), and N1769A (∇ , \blacktriangledown). Data for each experiment were normalized with respect to the largest control currents. The theoretical curves through control (dashed lines) and etidocaine conditions are least-squares fits of $a/[1 + \exp((V_H - V_{1/2})/k)]$, where a is a scaling factor, $V_{1/2}$ is the midpoint of the curve, and k is a slope factor. **(D)** Resting block as indicated by values for a determined from fits of the equation in (B) and (C) were plotted as a function of etidocaine concentration [Etid] for wild type (\bullet), I1761A (\blacktriangle), F1764A (\blacksquare), V1766A (\blacklozenge), and N1769A (\blacktriangledown). The theoretical curves are according to $(1/(1 + [\text{etid}]/K_r))$, where K_r is the midpoint of the dose-effect curve. **(E and F)** We replotted data in (B) (200 μM etidocaine) and in (C) (10 μM etidocaine) to demonstrate the shifts in $V_{1/2}$ caused by the drug. We normalized the data and theoretical curves in control and etidocaine conditions to the same maximum value and shifted them on the voltage axis until the control curves superimposed with $V_{1/2} = 0$ mV. **(G)** We determined block of inactivated channels for wild type (\bullet), I1761A (\blacktriangle), F1764A (\blacksquare), V1766A (\blacklozenge), and N1769A (\blacktriangledown) by stepping to -40 mV for 10 s and then giving a 10-ms recovery pulse to -110 mV, followed by a test pulse to 0 mV. The peak current evoked by the test pulse was normalized to control and plotted as a function of etidocaine concentration. The smooth line is according to $1 - (1/(1 + [\text{etid}]/K_r))$.



activation. This shift is a consequence of enhanced drug binding to inactivated channels (9, 10). To directly compare $\Delta V_{1/2}$ for wild type and mutants, we shifted curves in Fig. 1, B and C, obtained in the absence and in the presence of etidocaine along the voltage axis until the control curves superimposed, and the currents in the presence of drug were scaled to the same maximum value as that of the control (Fig. 1, E and F). For wild type, $\Delta V_{1/2}$ was about -7 mV in the presence of $10 \mu\text{M}$ etidocaine (Fig. 1F) and -24 mV with $200 \mu\text{M}$ etidocaine (Fig. 1E). The $\Delta V_{1/2}$'s for I1761A, V1766A (Fig. 1E), and N1769A (Fig. 1F) were approximately equal to those for wild type, indicating similarly strong drug binding to inactivated channels. In contrast, F1764A reduced $\Delta V_{1/2}$ to -7 mV (Fig. 1E), suggesting a decrease in the affinity of the inactivated channel.

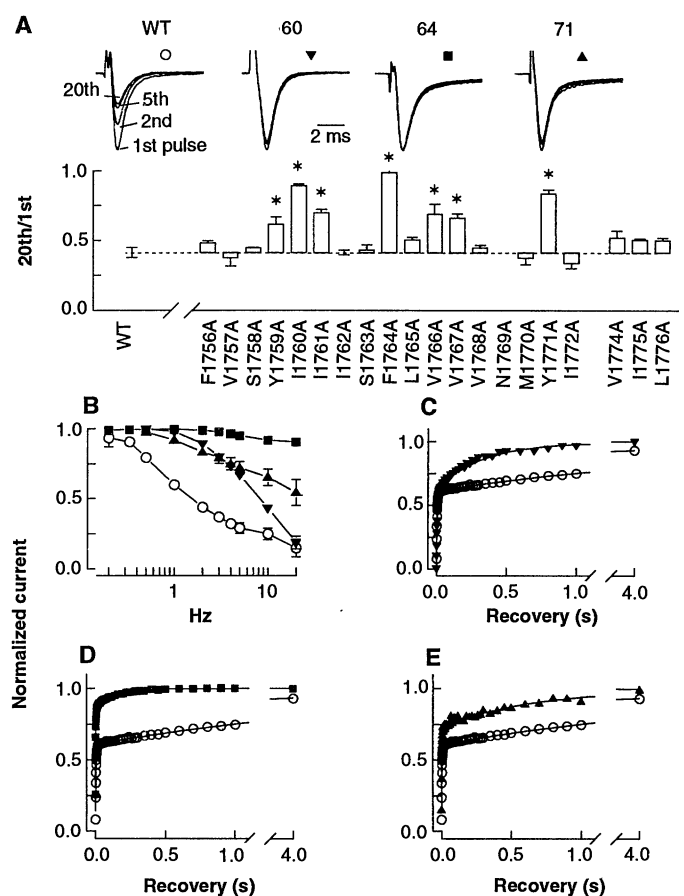
To examine drug binding to inactivated Na^+ channels directly (Fig. 1G), we first stepped the holding potential from -90 mV to -40 mV for 10 s, which inactivated most Na^+ channels but caused little channel activation. The long pulse duration ensured that drug binding to inactivated channels reached steady state. The membrane potential was then stepped to -110 mV for 10 ms, which allowed recovery of unblocked, fast-inactivated channels but which was short enough to prevent drug dissociation from most blocked channels. The availability of unblocked, resting channels was then assessed by a test pulse to 0 mV. In control conditions, this protocol caused a 40% reduction in current amplitude due to slow inactivation during the long conditioning prepulse, from which channels did not recover during the 10-ms repolarization (20). In the presence of the drug, there was an additional decrease in current amplitude due to drug binding to inactivated channels during the conditioning pulse. For wild type, this drug-dependent decrease in current was described by a 1:1 binding relation with a dissociation constant for inactivated channels (K_i) of $1 \mu\text{M}$ (Fig. 1G), $1/300$ of the value of K_r for binding to the resting state. The K_i 's for I1761A, V1766A, and N1769A were virtually identical to that for wild type (Fig. 1G). Thus, mutations that caused 3- to 15-fold increases in the affinity for the resting state had no detectable effect on K_i for binding to the inactivated state. In contrast, K_i for F1764A was $130 \mu\text{M}$ (Fig. 1G). Apparently the properties of the residue at this site are a determinant of tonic block due to drug binding to inactivated Na^+ channels.

Use-dependent block of Na^+ channels by local anesthetics during rapid trains of stimulus pulses results from binding of the drug to open and inactivated channels during depolarizing pulses and from slowed re-

Fig. 2. IVS6 mutations alter use-dependent block by etidocaine. (A) The histogram shows the ratios (mean \pm SEM; $n = 2$ to 22; *, $P < 0.05$) of the peak currents evoked by the 20th and 1st pulses in a 2-Hz pulse train in the presence of $200 \mu\text{M}$ etidocaine for wild-type (WT) and mutant channels. The traces above the graph are typical records showing currents elicited by the 1st, 2nd, 5th, and 20th pulses for the wild-type and selected mutants. (B) We assessed the dependence of use-dependent block on stimulus frequency for wild type (O), I1760A (\blacktriangledown), F1764A (\blacksquare), or Y1771A (\blacktriangle) channels by applying pulse trains of varying frequencies in the presence of $200 \mu\text{M}$ etidocaine. The mean ratios of the 20th/1st pulses were plotted as a function of stimulus frequency. (C through E) We examined channel recovery after depolarization-induced block by $200 \mu\text{M}$ etidocaine by giving a 15-ms conditioning pulse to 0 mV, followed by a recovery interval of varying duration at -90 mV and a test pulse to 0 mV. Peak test pulse current/peak conditioning pulse current was plotted as a function of the recovery interval. The graphs show typical experiments for I1760A (C, \blacktriangledown), F1764A (D, \blacksquare), and Y1771A (E, \blacktriangle), in each case compared with the same wild-type experiment (O). The smooth lines are least-squares fits of the sum of two exponentials.

covery of drug-bound channels between pulses. We assessed use-dependent block by applying 15-ms pulses to 0 mV at a frequency of 2 Hz in the presence of $200 \mu\text{M}$ etidocaine. For wild-type channels, this resulted in a further 60% use-dependent block of the Na^+ current that remained after the steady state for tonic block was reached (Fig. 2A, wild type). A number of mutations in IVS6 decreased use-dependent block in comparison to wild type. The largest decreases in use-dependent block were seen for the mutants I1760A, F1764A, and Y1771A (Fig. 2A).

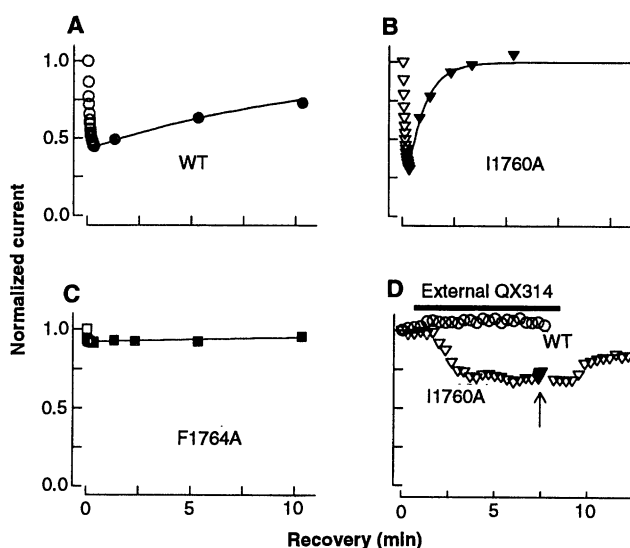
Use-dependent block of wild-type channels was just detectable when pulses were applied at 0.2 Hz, was half maximal at 1 to 2 Hz, and approached 100% at 20 Hz (Fig. 2B). Mutants I1760A, F1764A, and Y1771A exhibited less use-dependent block over this whole range of stimulus frequencies; however, the different mutants showed different frequency-dependence profiles. Use-dependent block in I1760A was dependent on frequency like wild type but was shifted to five times higher frequencies (Fig. 2B), whereas block in Y1771A was less frequency-dependent (Fig. 2B), and F1764A



was virtually insensitive to use-dependent block up to 20 Hz (Fig. 2B). These different profiles suggested that the mutations altered use-dependent block through different mechanisms.

In principle, mutations could alter use-dependent block during a pulse train either by altering the amount of drug that binds to open and inactivated channels during the depolarizing pulses or by altering the rate at which the drug dissociates between the pulses as the channels convert back to the resting state. We examined these parameters for wild-type, I1760A, F1764A, and Y1771A channels by determining the fraction of channels blocked during 15-ms conditioning pulses to 0 mV and the time course of recovery of these blocked channels after the holding potential was returned to -90 mV. Recovery in control conditions simply reflected the rate of recovery from fast inactivation, which was monoexponential, with a time constant of 2 to 6 ms at -90 mV (15). In the presence of $200 \mu\text{M}$ etidocaine, recovery had two kinetic components, one reflecting the fast recovery from inactivation of channels that were not blocked during the conditioning

Fig. 3. Block of wild-type and mutant channels by QX314. We studied the action of internally applied QX314 by microinjecting 50 nl of a 4 mM solution of QX314 in oocytes expressing (A) wild-type, (B) I1760, and (C) F1764 channels. We assumed an average oocyte volume of 1 μ l, so this resulted in an intracellular QX314 concentration of \sim 200 μ M. The oocytes were then voltage-clamped at -90 mV, and 10 min after microinjection, a 1-Hz train of 15-ms-long pulses to 0 mV was applied, resulting in use-dependent block (open symbols). We then assessed the rate of repriming at -90 mV by giving infrequent stimulus pulses (filled symbols). Each panel shows peak currents from a single experiment, normalized with respect to the current elicited by the first pulse in the train. The smooth lines through the recovery data are exponential fits. (D) Action of externally applied QX314. QX314 (500 μ M) was applied by superfusion to oocytes expressing wild-type (O) or I1760A (∇) channels for the time indicated by the bar. Currents were evoked by pulses applied at 20-s intervals. At the arrow, a 2-Hz pulse train was applied to the oocyte expressing I1760A channels. The data in each experiment were normalized with respect to the control currents.



cell membranes. They are ineffective when applied extracellularly but are potent use-dependent blockers when applied intracellularly (12, 13). These drugs act mainly on open Na⁺ channels through a cytoplasmic, hydrophilic pathway that is occluded by the activation and inactivation gates (9, 13, 14). Intracellularly applied QX314 was a use-dependent blocker of wild-type Na⁺ channels during a 1-Hz stimulus train (Fig. 3A). The time constant for recovery from QX314 block at -90 mV was approximately 12 min (Fig. 3A), which was 1/300 of the rate of recovery from etidocaine block. This slow recovery was probably caused by trapping of the charged drug when the activation or inactivation gates closed (13, 21, 22). I1760A displayed similar sensitivity to use-dependent block by QX314 (Fig. 3B); however, the time constant for recovery was only 0.8 min (Fig. 3B). Thus, complete recovery of I1760A channels blocked by QX314 took only a few minutes, as compared with more than 30 min for wild-type channels. The wild-type and I1760A channels exhibited similar voltage dependence for activation, indicating that the fast recovery of I1760A was not due to greater frequency of channel openings during the recovery intervals (21, 22). Apparently, the mutation created another pathway or lowered the energy barrier of an existing pathway for drug escape from closed channels.

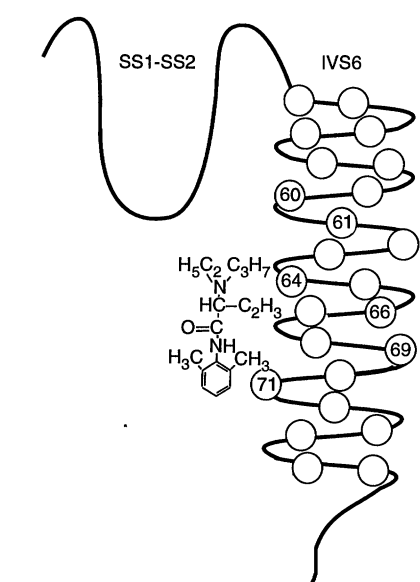


Fig. 4. Proposed orientation of amino acids in IVS6 with respect to a bound local anesthetic molecule in the ion-conducting pore. Segment SS1-SS2, which also contributes to the pore (27), is shown as well. Amino acids at positions 1760, 1764, and 1771 are shown facing the pore lumen.

About 40% of wild-type channels bound drug during the conditioning pulse, and these channels recovered with a time constant of 2.4 s (Fig. 2, C through E). For I1760A, the proportion of slowly recovering channels was almost identical to that for wild type (Fig. 2C), indicating that this mutation did not alter the affinity of the open or inactivated states for etidocaine. However, the recovery rate for drug-bound channels was eight times faster than for wild type. Thus, I1760A accelerated the escape of drug from closed channels at negative potentials, accounting for the altered frequency dependence of block.

In contrast to wild type and I1760A, only about 15% of the F1764A channels bound drug during the conditioning pulse, and the recovery of drug-bound channels was 20 times faster than for wild type (Fig. 2D). This indicates that the F1764A mutation reduced the affinity of open and fast inactivated channels for etidocaine, resulting in almost complete abolition of use-dependent block. This result is consistent with the high K_i value determined for F1764A (Fig. 1G). Y1771A also reduced drug binding during the conditioning pulse and speeded recovery of drug-bound channels (Fig. 2E), but the effect was less than for F1764A. Thus, Y1771A also reduced open or inactivated channel affinity but to a lesser extent. The K_i for Y1771A, determined by the conditioning pulse protocol in Fig. 1G, was 35 μ M.

Quaternary amines like QX314 are local anesthetic derivatives that are permanently positively charged and are impermeant to

cell membranes. They are ineffective when applied extracellularly but are potent use-dependent blockers when applied intracellularly (12, 13). These drugs act mainly on open Na⁺ channels through a cytoplasmic, hydrophilic pathway that is occluded by the activation and inactivation gates (9, 13, 14). Intracellularly applied QX314 was a use-dependent blocker of wild-type Na⁺ channels during a 1-Hz stimulus train (Fig. 3A). The time constant for recovery from QX314 block at -90 mV was approximately 12 min (Fig. 3A), which was 1/300 of the rate of recovery from etidocaine block. This slow recovery was probably caused by trapping of the charged drug when the activation or inactivation gates closed (13, 21, 22). I1760A displayed similar sensitivity to use-dependent block by QX314 (Fig. 3B); however, the time constant for recovery was only 0.8 min (Fig. 3B). Thus, complete recovery of I1760A channels blocked by QX314 took only a few minutes, as compared with more than 30 min for wild-type channels. The wild-type and I1760A channels exhibited similar voltage dependence for activation, indicating that the fast recovery of I1760A was not due to greater frequency of channel openings during the recovery intervals (21, 22). Apparently, the mutation created another pathway or lowered the energy barrier of an existing pathway for drug escape from closed channels.

Because I1760A is close to the extracellular side of IVS6, the mutation at this site might allow QX314 to escape from closed channels into the extracellular bath. If so, then this mutation would also create an access pathway for extracellular drug. To test this, we examined the action of extracellular QX314 on wild-type and I1760A channels. Bath-applied QX314 had no effect on wild-type channels (Fig. 3D) (12, 13); however, it rapidly blocked I1760A channels (Fig. 3D). Thus, mutation I1760A created an access pathway between the drug binding site and the extracellular medium that is normally occluded for quaternary drugs. This pathway probably also explains the rapid recovery of I1760A channels blocked by tertiary drugs. A 2-Hz train of pulses (Fig. 3D, arrow) applied after the drug did not produce use-dependent block of I1760A channels by extracellular QX314, suggesting that the extracellular pathway bypasses the channel gates, which regulate access through the intracellular pathway (9, 13, 14).

Intracellular QX314 produced almost no use-dependent block of F1764A channels (Fig. 3C). Because use-dependent block by internal QX314 occurs through open Na⁺ channels, this result provides further evidence that F1764A lowered the affinity of the open state for local anesthetics. The

small amount of block that did develop recovered slowly (Fig. 3C), like block of wild-type channels, indicating that F1764A did not alter the escape pathway, so the drug was trapped when the activation or inactivation gates closed.

Our results lead to a model of the local anesthetic receptor site in the pore of the Na⁺ channel. Mutations F1764A, Y1771A, and I1760A, which had the strongest effects on use-dependent block, are oriented on the same face of the IVS6 helix (Fig. 4). F1764A and Y1771A reduced open and inactivated channel affinity by one to two orders of magnitude, and F1764A also had a smaller effect on resting channel affinity, suggesting that the native residues at these positions contribute to the free energy of drug binding. F1764 and Y1771 are hydrophobic (23), aromatic residues separated by two turns of the S6 helix (Fig. 4), so they are about 11 Å apart. Effective local anesthetics are approximately 10 to 15 Å in length (24), with positively charged and hydrophobic moieties at either end that could interact with these residues through hydrophobic (25) or π electron (26) interactions. Therefore, we propose that F1764 and Y1771 are determinants of the local anesthetic binding site and that substitution of these residues with alanine destabilizes drug binding by reducing the hydrophobicity and aromaticity at these positions. I1760 is oriented on the same face of the helix as F1764 and Y1771 and is therefore well positioned to modulate extracellular access to the local anesthetic binding site. Replacement of the bulky isoleucine residue at position 1760 with alanine allows QX314 to reach the site from the extracellular medium, perhaps by passing directly through the pore from the outside. Thus, I1760 likely corresponds to a narrow region in the pore, just to the extracellular side of the local anesthetic binding site. The mutations I1761A, V1766A, and N1769A increased resting block without altering inactivated state affinity. Because these amino acids are oriented away from the face containing F1764, Y1771, and I1760 (Fig. 4), they may be oriented away from the channel pore. Mutations to alanine at these positions may increase channel sensitivity to drugs through indirect effects on the local anesthetic site, perhaps by partially inducing the inactivated binding site conformation in functionally resting Na⁺ channels.

REFERENCES AND NOTES

1. W. A. Catterall, *Physiol. Rev.* **72**, S15 (1992).
2. M. Noda *et al.*, *Nature* **320**, 188 (1986); T. Kayano, N. Noda, V. Flockerzi, H. Takahashi, S. Numa, *FEBS Lett.* **288**, 187 (1988).
3. V. J. Auld *et al.*, *Neuron* **1**, 449 (1988); V. J. Auld *et al.*, *Proc. Natl. Acad. Sci. U.S.A.* **87**, 323 (1990).
4. T. Scheuer *et al.*, *Science* **247**, 854 (1990).
5. J. W. West, T. Scheuer, L. Maechler, W. A. Catterall, *Neuron* **8**, 59 (1992).
6. M. Noda *et al.*, *Nature* **322**, 826 (1986); A. L. Goldin *et al.*, *Proc. Natl. Acad. Sci. U.S.A.* **83**, 7503 (1986).
7. L. L. Isom *et al.*, *Science* **256**, 839 (1992).
8. J. F. Butterworth IV and G. R. Strichartz, *Anesthesiology* **72**, 711 (1990); W. A. Catterall, *Trends Pharmacol. Sci.* **8**, 57 (1987).
9. B. Hille, *J. Gen. Physiol.* **69**, 497 (1977).
10. L. M. Hondeghem and B. G. Katzung, *Biochim. Biophys. Acta.* **427**, 373 (1977); B. P. Bean, C. J. Cohen, R. W. Tsien, *J. Gen. Physiol.* **81**, 613 (1983).
11. C. F. Starmer and K. R. Courtney, *Am. J. Physiol.* **251**, H848 (1986); C. F. Starmer, V. V. Nesterenko, F. R. Gilliam, A. O. Grant, *ibid.* **259**, H626 (1990).
12. D. T. Frazier, T. Narahashi, M. Yamada, *J. Pharm. Exp. Ther.* **171**, 45 (1970).
13. G. R. Strichartz, *J. Gen. Physiol.* **62**, 37 (1973); K. R. Courtney, *ibid.* **195**, 225 (1975).
14. M. Cahalan, *Biophys. J.* **23**, 285 (1978); ——— and W. Almers, *ibid.* **27**, 39 (1979).
15. D. S. Ragsdale, T. Scheuer, W. A. Catterall, *Mol. Pharmacol.* **40**, 756 (1991).
16. J. Striessnig, H. Glossman, W. A. Catterall, *Proc. Natl. Acad. Sci. U.S.A.* **88**, 9203 (1991); W. A. Catterall and J. Striessnig, *Trends Pharmacol. Sci.* **13**, 256 (1992); K. L. Choi, C. Mossman, J. Aubé, G. Yellen, *Neuron* **10**, 533 (1993); G. E. Kirsch, C. C. Shieh, J. A. Drew, D. F. Vener, A. M. Brown, *ibid.* **11**, 503 (1993).
17. D. E. Patton, J. W. West, W. A. Catterall, A. L. Goldin, *Proc. Natl. Acad. Sci. U.S.A.* **89**, 10905 (1992).
18. Experimental conditions for the mutagenesis of IVS6, for its injection, and for the electrophysiological recording of *Xenopus* oocytes have been described [J. C. McPhee *et al.*, *Proc. Natl. Acad. Sci. U.S.A.*, in press]. Abbreviations for the amino acid residues are as follows: A, Ala; C, Cys; D, Asp; E, Glu; F, Phe; G, Gly; H, His; I, Ile; K, Lys; L, Leu; M, Met; N, Asn; P, Pro; Q, Gln; R, Arg; S, Ser; T, Thr; V, Val; W, Trp; and Y, Tyr. Each amino acid is indicated by its one-letter code. The number indicates its position in the chain, and A at the end indicates that alanine has been substituted for the native amino acid. Except where noted by error bars, the data presented in the figures are single examples from three or more experiments that led to the same conclusion.
19. J. S. Richardson, *Adv. Protein Chem.* **34**, 167 (1981); M. Blaber, K. J. Zhang, B. W. Matthews, *Science* **260**, 1637 (1993).
20. W. J. Adelman and Y. Palti, *J. Gen. Physiol.* **54**, 589 (1969); W. K. Chandler and H. Meves, *J. Physiol. (London)* **211**, 707 (1970); J. M. Fox, *Biochim. Biophys. Acta* **426**, 232 (1976); T. Brismar, *J. Physiol. (London)* **270**, 283 (1977); B. Rudy, *ibid.* **283**, 1 (1978); F. N. Quandt, *ibid.* **392**, 563 (1987).
21. J. Z. Yeh and J. Tanguy, *Biophys. J.* **47**, 685 (1985).
22. C. F. Starmer, J. Z. Yeh, J. Tanguy, *ibid.* **49**, 913 (1986).
23. T. P. Hopp and K. R. Woods, *Proc. Natl. Acad. Sci. U.S.A.* **78**, 3824 (1981).
24. K. R. Courtney, *J. Mol. Cell. Cardiol.* **20**, 465 (1988).
25. P. M. Bokesh, C. Post, G. R. Strichartz, *J. Pharm. Exp. Ther.* **237**, 773 (1986); R. S. Sheldon, R. J. Hill, M. Taouis, L. M. Wilson, *Mol. Pharmacol.* **39**, 609 (1991); G. W. Zamponi and R. J. French, *Biophys. J.* **65**, 2335 (1994).
26. L. Heginbotham and R. MacKinnon, *Neuron* **8**, 483 (1992).
27. S. H. Heinemann, H. Terlau, W. Stühmer, K. Imoto, S. Numa, *Nature* **356**, 441 (1992); P. H. Backx, D. T. Yue, J. H. Lawrence, E. Marban, G. F. Tomaselli, *Science* **257**, 248 (1992).
28. Supported by research grants R01-NS15751 and P01-HL44948 from the NIH (to W.A.C.), postdoctoral fellowships from the NIH (to D.S.R. and J.C.M.), and the W. M. Keck Foundation.

1 June 1994; accepted 8 August 1994

Role of a Conserved Retinoic Acid Response Element in Rhombomere Restriction of *Hoxb-1*

Michèle Studer, Heike Pöpperl, Heather Marshall, Atsushi Kuroiwa, Robb Krumlauf*

After activation in mesoderm and neuroectoderm, expression of the *Hoxb-1* gene is progressively restricted to rhombomere (r) 4 in the hindbrain. Analysis of the chick and mouse *Hoxb-1* genes identified positive and negative regulatory regions that cooperate to mediate segment-restricted expression during rhombomere formation. An enhancer generates expression extending into r3 and r5, and a repressor limits this domain to r4. The repressor contains a conserved retinoic acid response element, point mutations in which allow expression to spread into adjacent rhombomeres. Retinoids and their nuclear receptors may therefore participate in sharpening segment-restricted expression of *Hoxb-1* during rhombomere boundary formation.

Rhombomeres are segmental units of organization in the vertebrate hindbrain (1). Cell mixing can occur between prospective neighboring segments before rhombomeres become lineage-restricted cellular compartments (2). Later, boundaries form between

odd- and even-numbered units; however, cells can mix when even- or odd-numbered rhombomeres are grafted adjacent to each other, which suggests that the formation and maintenance of boundaries are dependent on signaling between odd and even segments (3). Some of the *Hox* homeobox genes important for regulating axial patterning have limits of expression that coincide with rhombomere boundaries (4, 5). For example, expression of the *Hoxb-1* gene is progressively restricted to r4 in the hindbrain (4, 6–8). These patterns of expression, combined with mutational analysis (9,

M. Studer, H. Pöpperl, H. Marshall, R. Krumlauf, Lab of Developmental Neurobiology, National Institute for Medical Research, The Ridgeway, Mill Hill, London NW7 1AA, UK.

A. Kuroiwa, Department of Molecular Biology, School of Science, Nagoya University, Chihusa-Ku, Nagoya, Japan 464-01.

*To whom correspondence should be addressed.